

Ground state properties of a Tonks-Girardeau Gas in a periodic potential

Bo-Bo Wei, Shi-Jian Gu, and Hai-Qing Lin

*Department of Physics and Institute of Theoretical Physics,
The Chinese University of Hong Kong, Hong Kong, China*

(Dated: November 5, 2018)

In this paper, we investigate the ground-state properties of a bosonic Tonks-Girardeau gas confined in a one-dimensional periodic potential. The single-particle reduced density matrix is computed numerically for systems up to $N = 265$ bosons. Scaling analysis of the occupation number of the lowest orbital shows that there are no Bose-Einstein Condensation (BEC) for the periodically trapped TG gas in both commensurate and incommensurate cases. We find that, in the commensurate case, the scaling exponents of the occupation number of the lowest orbital, the amplitude of the lowest orbital and the zero-momentum peak height with the particle numbers are 0, -0.5 and 1, respectively, while in the incommensurate case, they are 0.5, -0.5 and 1.5, respectively. These exponents are related to each other in a universal relation.

PACS numbers: 03.75.Lm, 05.30.Jp, 03.75.Hh

I. INTRODUCTION

With the development of optical lattices and atom chip traps, quasi-one-dimensional cold atom systems have been realized by tightly confining the particle's motion in two directions to zero-point oscillation [1–3]. Meanwhile, by using the Feshbach resonance or tuning the effective mass of particles moving in a periodic potential [1, 4], the inter-particle scattering length can be tuned to almost any value desired. These progresses have led to experimental realizations of the one-dimensional (1D) exactly solvable model that describes an interacting Bose gas [5–8].

At very low temperatures and densities, a 1D Bose gas is expected to behave as a gas of impenetrable particles known as hard-core bosons [9–11]. In particular, two recent experiments successfully achieved the so-called Tonks-Girardeau (TG) regime and made the TG gas a physical reality [1, 2]. Physically, a TG gas is defined to be a 1D strongly correlated quantum gas consisting of bosons with hardcore interaction. This model of a 1D Bose gas was first proposed by Tonks in 1936 [12]. As a milestone development to the model, Girardeau solved the model exactly by the famous Bose-Fermi mapping [5, 8, 13], where the TG gas has been mapped to a spinless free fermion gas. Recently, it was found that the above case is just a special case of a general mapping theorem between bosons and fermions in one dimension, where the particles can interact with finite strength [14, 15].

Since the TG gas is both theoretical exactly solvable and experimentally accessible, there are great research interests recently in the TG gas with different trapping potentials [16–32]. A review on relevant studies in this interesting subject can be found in a recent article by Yukalov and Girardeau [13]. In particular, Lin and Wu investigated the ground-state properties of a TG in periodic potentials [28]. They used a Monte Carlo integration technique to compute the single-particle reduced density matrix (SPRDM) for systems up to $N = 7$ bosons. Their analysis of the ground state shows that when the number

of bosons N is commensurate with the number of wells M in the periodic potential, the boson system is a Mott insulator whose energy gap is given by the single-particle band gap of the periodic potential; however, when N is not commensurate with M , the system is a metal (not a superfluid). The purpose of this work is to compute the SPRDM for large systems containing more than 200 particles, and then study scaling relations, make quantitative predictions for scaling exponents of the ground-state occupation numbers, and obtain zero-momentum peak in different phases. We put particular emphasis on examining the ground-state occupation in the two phases of the system.

The remaining of this paper is organized as follows. In Sec. II, we introduce the model Hamiltonian of the system and describe the single-particle eigenstates and eigenvalues which will be used. In Sec. III, we apply the Bose-Fermi mapping theorem to construct the exact many-body ground state wave function. In Sec. IV, we devote ourselves to study the many-body properties of the TG gas. Finally, summary and conclusions are given in Sec. V.

II. MODEL HAMILTONIAN AND SINGLE-PARTICLE EIGENSTATES

A. Model Hamiltonian

We consider a gas of N hardcore bosons trapped in a tight atomic waveguide. The waveguide restricts strongly the dynamics of the gas in the transversal directions, such that in the low temperature limit we can define our model in the longitudinal direction only. In this direction we consider a periodic potential such that the many-particle Hamiltonian at low density can be written as

$$H = \sum_{j=1}^N \left[-\frac{\hbar^2}{2m} \frac{\partial^2}{\partial x_j^2} + V(x_j) \right], \quad (1)$$

where m is the mass of a single boson, $V(x) = V(x + d)$, the periodic potential with d being the period. In this work, we use the Kronig-Penney (KP) potential as a candidate for the periodic potential, which takes the form

$$V(x) = \gamma' \sum_{j=1}^M \delta(x - jd) \quad (2)$$

where γ' is the strength of the δ -function potential and M is the total number of periodic wells.

B. Eigenstates and eigenvalues of periodic potential

We impose the usual periodic boundary conditions and use d as the unit of distance and $\hbar^2/(2md^2)$ as the unit of energy. Then we arrive at the following dimensionless single-particle Hamiltonian,

$$H = -\frac{\partial^2}{\partial x^2} + \gamma \sum_{j=1}^M \delta(x - jd). \quad (3)$$

where $\gamma = 2md^2\gamma'/(\hbar^2d)$. This single-particle Hamiltonian can be solved exactly. We review the result for later computation. The Bloch wave functions take the form

$$\begin{aligned} \psi_\alpha(x) &= C_\alpha [\sin(k_\alpha x) + e^{-iK_\alpha} \sin[k_\alpha(1-x)]], 0 \leq x \leq 1, \\ \psi_\alpha(x) &= e^{iK_\alpha[x]} \psi_\alpha(x - [x]), 1 \leq x \leq M. \end{aligned} \quad (4)$$

The eigenenergy is

$$E_\alpha = k_\alpha^2 \quad (5)$$

where k_α satisfies the transcendental equation

$$\cos(k_\alpha) + \gamma \frac{\sin(k_\alpha)}{2k_\alpha} = \cos(K_\alpha), \quad (6)$$

with

$$K_\alpha = \frac{2\pi\alpha}{M}, \quad \alpha = 0, \pm 1, \pm 2, \dots, \pm \frac{M-1}{2}. \quad (7)$$

and the normalization constant for the Bloch wave function is given by

$$C_\alpha = \sqrt{\frac{k_\alpha}{M[k_\alpha - \frac{1}{2} \sin(2k_\alpha) + \cos K_\alpha (\sin k_\alpha - k_\alpha \cos k_\alpha)]}}. \quad (8)$$

III. BOSE-FERMI MAPPING THEOREM AND MANY-BODY WAVE FUNCTIONS OF THE TG GAS

For a system of N identical hardcore bosons in the 1D external potential $V(x)$, the bosons interact with each

other by impenetrable pointlike interactions, which can be more conveniently treated as a boundary condition for the many-body wave function $\Psi_B(x_1, x_2, \dots, x_N, t)$:

$$\Psi_B(x_1, x_2, \dots, x_N, t) = 0 \text{ if } x_i = x_j, 1 \leq i < j \leq N. \quad (9)$$

Then the hardcore boson gas can be considered as a free boson gas governed by the following free Schrödinger equation,

$$i \frac{\partial}{\partial t} \Psi_B = \sum_{j=1}^N \left[-\frac{\partial^2}{\partial x_j^2} + V(x_j) \right] \Psi_B, \quad (10)$$

where the wave function Ψ_B satisfies the hardcore boundary condition of Eq. (9). Based on the observation that the hardcore boundary condition of Eq. (9) is automatically satisfied by a wave function of fermions due to its antisymmetry, Girardeau [5, 8] gave the exact many-body wave function of the hardcore boson system via the famous Bose-Fermi mapping, which relates the wave function of hardcore bosons to that of noninteracting spinless fermions in the same trapping potential:

$$\Psi_B(x_1, x_2, \dots, x_N) = A \Psi_F(x_1, x_2, \dots, x_N, t). \quad (11)$$

with

$$A = \prod_{1 \leq i < j \leq N} \text{sgn}(x_i - x_j), \quad (12)$$

where sgn is sign function and A is unit antisymmetric function which ensures that Ψ_B has proper symmetry under the exchange of two bosons. The free fermionic wave function can be compactly written in a form of the Slater determinant

$$\Psi_F = \frac{1}{\sqrt{N!}} \text{Det}_{m,j=1}^N [\psi_m(x_j, t)]. \quad (13)$$

where $\{\psi_m\}, m = 1, \dots, N$ are the single-particle eigenstates. These eigenstates are governed by a set of uncoupled single-particle Schrödinger equations,

$$i \frac{\partial}{\partial t} \psi_m(x) = \left[-\frac{\partial^2}{\partial x^2} + V(x) \right] \psi_m(x). \quad (14)$$

Eqs. (11),(13) and (14) describe how to construct the exact many-body wave functions of a TG gas in any external potential $V(x)$. Then the wave function of the TG gas is

$$\Psi_B = A(x_1, x_2, \dots, x_N) \frac{1}{\sqrt{N!}} \text{Det}_{m,j=1}^N [\psi_m(x_j, t)]. \quad (15)$$

where $\psi_m(x)$ is the single-particle eigenstate in the trapping potential $V(x)$.

In the Bose-Fermi mapping, the many-body ground state of hardcore bosons is mapped from the many-body ground state of noninteracting spinless fermions in the same trapping potential [5, 8]. So to construct the ground

state wave function of a TG gas, one should choose lowest N single-particle eigenstates in the Slater determinant of Eq. (15). For the periodic potential that we are considering in this work, the single-particle eigen functions are given by Eq. (4), then we can construct the exact many-body ground state wave function of the TG gas in the KP potential according to the above procedures. The ground-state many-body properties of the TG gas in the KP potential can be extracted from this exact wave function.

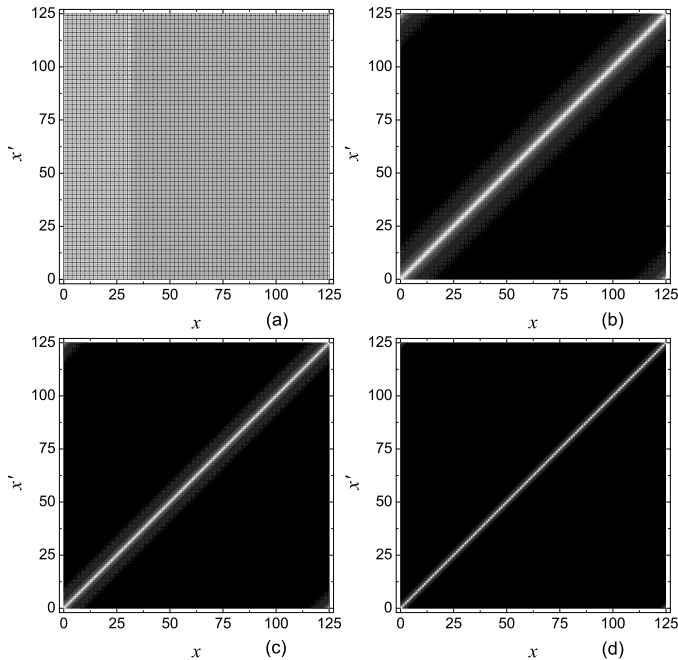


FIG. 1: Single-particle reduced density matrix, $\rho(x, x')$, of the TG gas in periodic potential for different particle numbers, (a) $N = 1$, (b) $N = 45$, (c) $N = 85$, (d) $N = 125$ when the number of periodic wells $M = 125$. All lengths are in units of the period of the periodic potential d .

IV. MANY-BODY PROPERTIES OF TG GAS IN PERIODIC POTENTIALS

In this section we investigate the ground-state properties of the 1D TG gas in the periodic potential using the exact ground state many-body wave function of the previous section.

A. Single-particle reduced density matrix

The many-body wave function Ψ_B fully describes the state of the system. However, its form does not transparently yield physical information related to many important observables such as occupation numbers of natural

orbitals and the momentum distributions. The expectation value of one-body observables are readily obtained from the SPRDM,

$$\rho(x, x') = N \int dx_2 \cdots dx_N \Psi_B^*(x, x_2, \dots, x_N) \times \Psi_B(x', x_2, \dots, x_N), \quad (16)$$

Its diagonal elements are the position density distribution, which satisfies the normalization condition

$$\int \rho(x, x) dx = N \quad (17)$$

Although the exact many-body wave function of the TG gas can be written in a compact form, the calculation of the SPRDM is a difficult task as it is very time consuming to calculate multidimensional integrals in SPRDM for a large system [18–25, 33, 34]. However, in the TG limit the SPRDM can be written in a matrix product form in terms of single-particle eigenstates [29]

$$\rho(x, x') = \sum_{i,j=1}^N \psi_i^*(x) A_{ij}(x, x') \psi_j(x'). \quad (18)$$

Here the $N \times N$ matrix $\mathbf{A}(x, x') = \{A_{ij}(x, x')\}$ takes the form,

$$\mathbf{A} = (\mathbf{P}^{-1})^T \text{Det } \mathbf{P} \quad (19)$$

where the entries of the matrix \mathbf{P} are $P_{ij}(x, x') = \delta_{i,j} - 2 \int_x^{x'} \psi_i^*(t) \psi_j(t) dt$, and we can assume $x < x'$ without loss of generality.

In addition, we observe that the SPRDM in the periodic potential we are considering satisfies

$$\rho(x+1, x'+1) = \rho(x, x'), \quad (20)$$

which can be easily derived from the properties of Bloch wave functions. These formalism of the SPRDM enable us to calculate considerable large systems of the TG gas.

The SPRDM expresses self-correlation and one can view $\rho(x, x')$ as the probability that, having detected the particle at position x , a second measurement, immediately following the first, will find the particle at the position x' . Classically, $\rho(x, x') = \delta(x - x')$, so the off diagonal elements of SPRDM come from purely quantum correlations of the particles. Fig. 1 displays contour plots of SPRDM, $\rho(x, x')$, for different number of particles $N = 1, 45, 85$ and 125 respectively, where the number of wells of the periodic potential $M = 125$. We clearly see a characteristic pattern for each value of N : The SPRDM are largest close to the diagonal elements which stands for the position density distributions. The diagonal elements of SPRDM shows oscillations due to the barrier of the periodic potential which tends to repel the particles and push the particles stay inside the well. The off-diagonal elements of the SPRDM relate to off-diagonal long-range order (ODLRO) [35, 36] and we

can see that the off-diagonal elements are decreasing in contrast to the diagonal as the number of particles N increases. It means that the repulsive interaction tends to destroy off-diagonal coherence, so there is no ODLRO for a system of hard core bosons in a 1D periodic potentials in the thermodynamic limit. As $N = M$, the SPRDM is almost diagonal and the system has diagonal long range order while lacks ODLRO. This is because the system is a Mott-insulator phase in the commensurate case where all the particles are localized. In this case, we can approximate the SPRDM as $\rho(x, x') \simeq \rho(x, x)\delta(x - x')$, which will be used in the following sections to predict some interesting results.

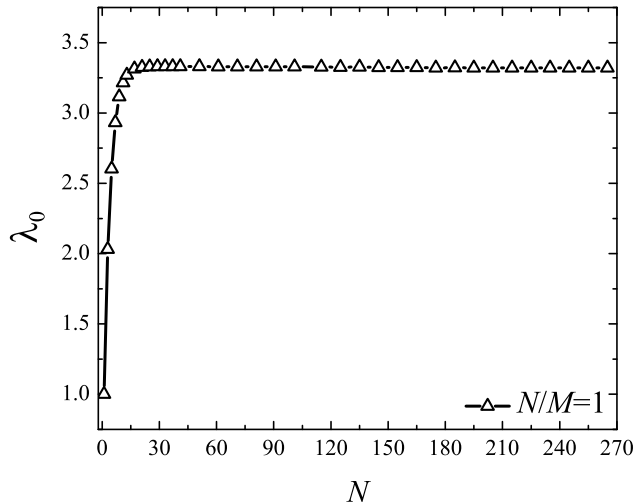


FIG. 2: Occupation numbers of the lowest orbital λ_0 as a function of particle number N in the commensurate case, $N/M = 1$, when the periodic potential strength $\gamma = 2$.

B. Occupation numbers and natural orbital

The occupation numbers and the natural orbitals are defined from the SPRDM,

$$\int dx' \rho(x, x') \phi_i(x') = \lambda_i \phi_i(x), i = 0, 1, \dots, \quad (21)$$

where $\phi_i(x), i = 0, 1, 2, \dots$ are the so called natural orbitals, which are the eigenfunctions of the SPRDM and they represent effective single-particle states. Generally, the natural orbitals are different from the single-particle eigenstates. Unless there are some special reasons, such as translation invariance, the single-particle eigenstates and natural orbitals are the same plane-wave momentum eigenstates. In trapped systems, there is no simple relation between them. The corresponding eigenvalue λ_i is the occupation number of the i -th natural orbital. The eigenvalue of each orbital gives the population probability of that orbital and summation of the occupation numbers of all the orbitals satisfies $\sum_i \lambda_i = N$.

The SPRDM is diagonal in the basis of natural orbitals, $\rho(x, x') = \sum_i \lambda_i \phi_i^*(x) \phi_i(x')$. The natural orbitals can be labelled in a descending order according to their eigenvalues, $\lambda_0 > \lambda_1 > \lambda_2 \dots$.

In a macroscopic interacting system, the existence of ODLRO is determined by the behavior of $\rho(x, x')$ as $|x - x'| \rightarrow \infty$ [35, 36]. ODLRO is present if the largest eigenvalue of $\rho(x, x')$ is macroscopically non-vanishing (proportional to N). Which means a macroscopic number of particles will condense to the lowest orbital. In this case the system exhibits BEC and the corresponding eigenfunction, the condensate orbital, plays the role of an order parameter. The fraction of particles that are in the orbital is related to the largest eigenvalue of the SPRDM by $f_0 = \lambda_0/N$. Therefore, in analogy to the macroscopic occupation of a single-particle eigenstate in the BEC of non-interacting Bose gas, this orbital is sometimes referred to as the ‘‘BEC’’ state and the occupation number hence acts as a measure of the coherence in the system.

For the TG gas in periodic potentials, there are two different phases in the ground state [28]. One is a Mott-insulator for the commensurate case where N/M is an integer. In this phase, one or more Bloch bands have been fully occupied. The other one is a boson conductor phase for the incommensurate case where N/M is a fractional number. In this phase, the Bloch bands are partially occupied. What we are interested in here is the scaling behavior of the occupation number of lowest orbital in different phases. Diagonalizing the SPRDM numerically, we can obtain the occupation numbers of the lowest orbital for different system sizes.

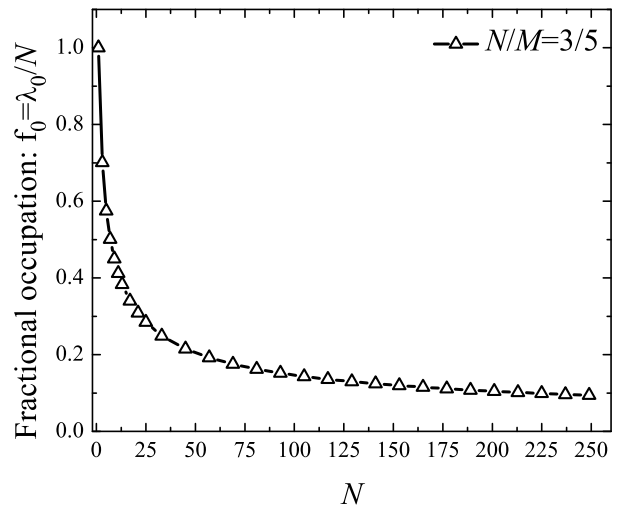


FIG. 3: Fractional occupations of the lowest orbital, $f_0 = \lambda_0/N$, as a function of particle number N , in the incommensurate case, $N/M = 3/5$, when the periodic potential strength $\gamma = 2$.

We have shown the occupation number of the lowest orbital, λ_0 , with particle numbers N , in the commen-

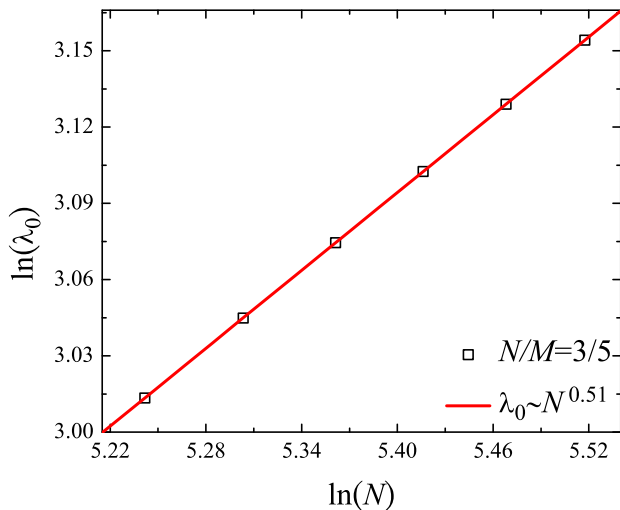


FIG. 4: (Color online) Finite size scaling analysis of the occupation number of the lowest orbital in the incommensurate case, $N/M = 3/5$, when the periodic potential strength $\gamma = 2$.

surate case (the lowest Bloch band has been fully occupied) when $\gamma = 2$ in Fig. 2. From the figure, we observe that the occupation number of the lowest orbital increases with the increase of the system size initially and then saturate to a constant as the particle number increases further. So the occupation number of the lowest orbital shows $\lambda_0 \sim N^\alpha$ with $\alpha = 0$ in the Mott-insulating phase. The zero-exponents of the occupation numbers of the lowest orbital can also be derived from the approximation, $\rho(x, x') \simeq \rho(x, x)\delta(x - x')$. From Eq.(21), we have

$$\int dx' \rho(x, x)\delta(x - x')\phi_i(x') = \lambda_i \phi_i(x), \quad (22)$$

$$\rho(x, x)\phi_i(x) = \lambda_i \phi_i(x), \quad (23)$$

$$\rho(x, x) = \lambda_i. \quad (24)$$

where $\rho(x, x)$ is the position density distribution, which are the same for the TG gas and its fermionic counterpart,

$$\rho(x, x) = \sum_i |\psi_i(x)|^2. \quad (25)$$

Then we have

$$\lambda_0 = \text{Max}\{\rho(x, x)\}. \quad (26)$$

The position density distributions satisfy $\int \rho(x, x)dx = N$. Meanwhile, the position density distributions are periodic with period of 1 in the periodic potential, which can be clearly observed from Fig. 1. So the position density distributions are normalized inside each well, which is independent of the system size in the commensurate case. Then the maximum of $\rho(x, x)$ is also independent of the system size, $\text{Max}\{\rho(x, x)\} \sim N^0$. Thus we have

$$\lambda_0 \sim N^0. \quad (27)$$

So this confirms our numerical result, $\lambda_0 \sim N^0$, which is shown in Fig. 2, in the Mott-insulating phase. Thus we can infer that there is no BEC for the periodically trapped TG gas in the commensurate case.

The fractional occupation of the lowest orbital, $f_0 = \lambda_0/N$, as a function of particle number N , in the incommensurate case, $N/M = 3/5$, and $\gamma = 2$ is displayed in Fig. 3. We see that the fractional occupation of the lowest orbital in the incommensurate case decreases with the increases of the particle number and will vanish in the thermodynamic limit. Doing finite size scaling of the occupation number of the lowest orbital in Fig. 4, from which we find that the occupation numbers of the lowest orbital λ_0 shows power law dependence on the particle number N of the system in the incommensurate case, i.e $\lambda_0 \sim N^\alpha$ with $\alpha = 0.51$ for the number of particles up to $N = 249$. In Table I, we have made a list of the best converged exponents and the number of particles involved. Simple scaling arguments presented below show that the exponents will converge to 0.5 in the thermodynamic limit. This behavior of periodically trapped hard-core bosons in the incommensurate case is similar to the uniform system of hard-core bosons [25, 33] and harmonically trapped hardcore bosons [24, 25]. So there is also no BEC behavior for periodically trapped hardcore bosons in the incommensurate case.

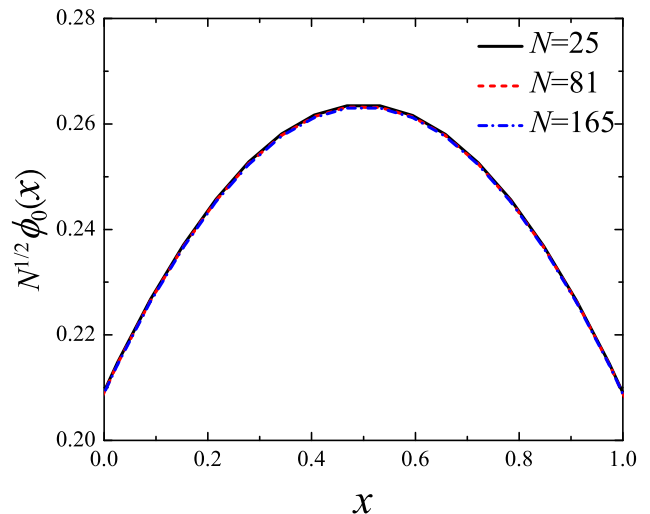


FIG. 5: (Color online) Scaled lowest natural orbital $\sqrt{N}\phi_0(x)$ for $N = 25$ (full line), $N = 81$ (dashed line), and $N = 165$ (dashed-dotted line) bosons in the incommensurate case, $N/M = 3/5$, when the periodic potential strength $\gamma = 2$. The amplitude of the lowest natural orbitals are in units of $1/\sqrt{d}$ and the length is in units of the period of the periodic potential d .

We display the scaled lowest natural orbital $\sqrt{N}\phi_0(x)$ for $N = 25, 81, 165$ in the incommensurate case in Fig. 5. The lowest natural orbital in the incommensurate case are periodic with period of 1, so we show the natural orbitals in one period only. We observe that the scaled

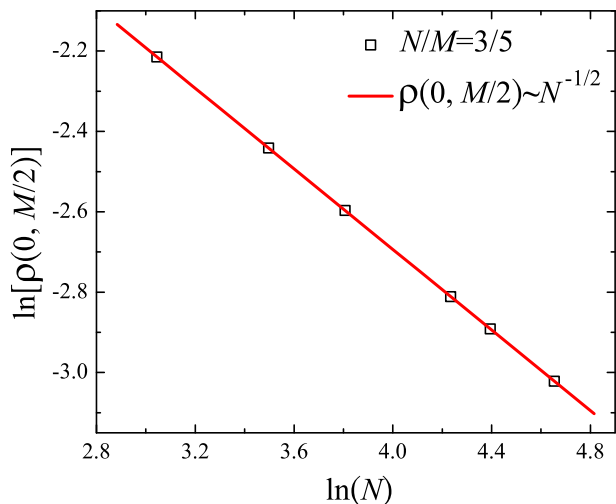


FIG. 6: (Color online) Off-diagonal element $\rho(0, M/2)$ as a function of particle number N in the incommensurate case, $N/M = 3/5$, when periodic potential strength $\gamma = 2$. The off-diagonal element $\rho(0, M/2)$ is in units of the inverse of the period of the periodic potential $1/d$.

lowest natural orbitals are N -independent function that depends only on the variable x as N increases. We find that the amplitude of the lowest natural orbital in the incommensurate case scales as $\phi_0(x) \propto N^\beta$ with $\beta = -0.5$. This scaling behavior is expected as the natural orbitals are normalized and extend from 0 to M (in the order of N). Similarly, the lowest natural orbital in the commensurate case is also periodic with period of 1 due to the presence of periodic potential. The natural orbitals are all normalized, $\int |\phi_0(x)|^2 dx = 1$, then the amplitude of the lowest orbital also scales as $\phi_0(x) \propto N^\beta$ with $\beta = -0.5$ in the commensurate case.

The scaling behavior of diagonal elements of SPRDM is N^0 , as $\int \rho(x, x) dx = N$ and x extends over an interval in the order of N . We know the off-diagonal elements qualitatively decrease as N increases from Fig. 1, to see this more clearly, we do finite size scaling of the off-diagonal elements, $\rho(0, M/2)$, of SPRDM in Fig. 6. It is clear from the figure that, with the increases of the particle number N , the interaction in the system gets stronger, then the off-diagonal element decreases. This indicates that the interaction suppresses the off-diagonal terms. Secondly, we find that off-diagonal element scales as $\rho(0, M/2) \propto N^{-1/2}$ with the particle number N .

These findings are particularly interesting, because they allow us to predict the scaling behavior of the occupation number of the lowest orbital λ_0 in the incommensurate case. From Eq.(21), we have

$$\begin{aligned} \lambda_0 \phi_0(0) &= \int \rho(0, x') \phi_0(x') dx' \sim N^{-0.5} N^{-0.5} \times N \\ &\sim N^0 \end{aligned} \quad (28)$$

where $\phi_0(0)$ is non-zero as the finite strength of the pe-

riodic potential we are considering, which also scales as $\phi_0(0) \sim N^{-0.5}$. Therefore, we have obtained the scaling behavior of the occupation number of the lowest orbital in the incommensurate case,

$$\lambda_0 \sim \sqrt{N}. \quad (29)$$

Number of particles N	Scaling exponents α ($\lambda_0 \sim N^\alpha$)
25	0.56
45	0.54
105	0.52
249	0.51
∞	0.5

TABLE I: Comparison of best converged scaling exponents of the occupation number of the lowest natural orbital in the incommensurate case and particle number involved.

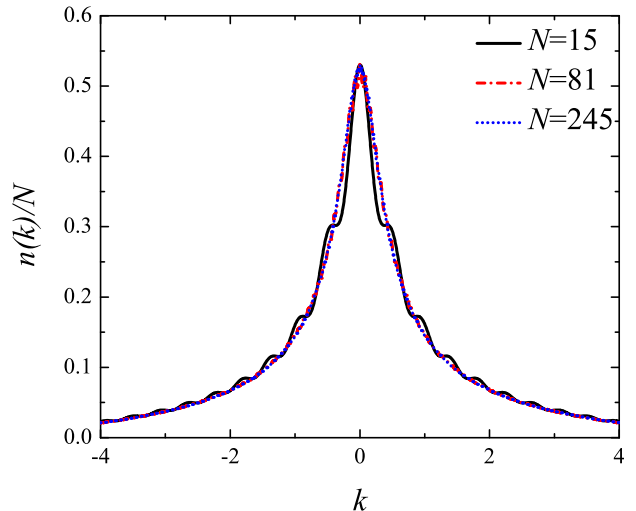


FIG. 7: (Color online) Normalized momentum density distributions for $N = 15$ (solid line), $N = 81$ (dashed-dotted line) and $N = 245$ (dotted line) bosons in the commensurate case, $N/M = 1$, when the periodic potential strength $\gamma = 2$. The momentum k is given in units of the inverse of the period of the periodic potential, $1/d$, and the momentum density is in units of the period of the periodic potential d .

C. Momentum density distribution

Although the position density profiles and energy spectrum are exactly the same between the hardcore boson gas and its corresponding spinless free fermion gas due to Bose-Fermi mapping theorem, the momentum density distributions differ considerably from each other [28, 32]. The momentum density distributions can be obtained from the SPRDM as

$$n(k) = (2\pi)^{-1} \int dx dx' \rho(x, x') e^{-ik(x-x')}. \quad (30)$$

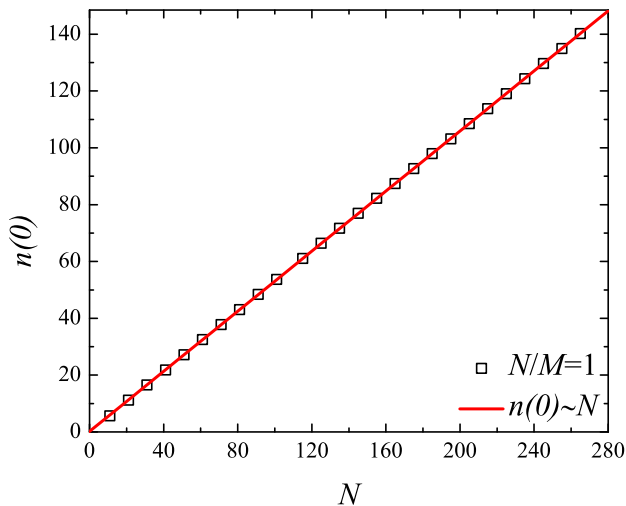


FIG. 8: (Color online) Zero-momentum peak, $n(0)$, as a function of particle number N in the commensurate case, $N/M = 1$, when the periodic potential strength $\gamma = 2$. $n(0)$ is in units of the period of the periodic potential d .

Obviously, the momentum density distributions satisfy

$$\int n(k)dk = N. \quad (31)$$

The normalized momentum density distributions of periodically trapped TG gas in the commensurate case are shown in Fig. 7 for various particle numbers. We see that the normalized momentum density distributions of the TG gas has a bosonic structure, which has peaks at $k = 0$ and the profiles are narrow. While its fermionic counterpart, the spinless free fermion gas, has a broad Fermi momentum distributions. Although a TG gas has the same energy spectrum and position profiles with its fermionic counterpart, their momentum distributions are very different. In addition, the profiles of normalized momentum distributions are nearly unchanged with the increase of the system sizes in the commensurate case. This is because the periodically trapped TG gas in the commensurate case is a Mott-insulating phase, so particles are localized in the real space. In the language of matter waves, the wave packages of the particles have no overlapping. With the increase of system size, the particles do not affect each other in any essential way. The oscillations in the momentum density distributions come from the finite size effect, it will vanish in the thermodynamic limit. What is more interesting here is that we find the momentum density distributions have same zero momentum peaks after rescaling. Then we plot $n(0)$ as a function of particle number N in Fig. 8. It clearly shows that $n(0) \propto N^\gamma$ with $\gamma = 1$ in the commensurate case. Similar behavior has been found for the TG gas in the harmonic trap [24]. In the commensurate case, which is the Mott-insulating phase, we can approximate the SPRDM as $\rho(x, x') \simeq \rho(x, x)\delta(x - x')$, then the zero-

momentum density can be obtained as

$$n(0) = (2\pi)^{-1} \int dx dx' \rho(x, x') \quad (32)$$

$$\simeq (2\pi)^{-1} \int dx dx' \rho(x, x)\delta(x - x') \quad (33)$$

$$\simeq (2\pi)^{-1} \int dx \rho(x, x) \quad (34)$$

$$\simeq (2\pi)^{-1} N \quad (35)$$

which confirms our numerical result shown in Fig. 8.

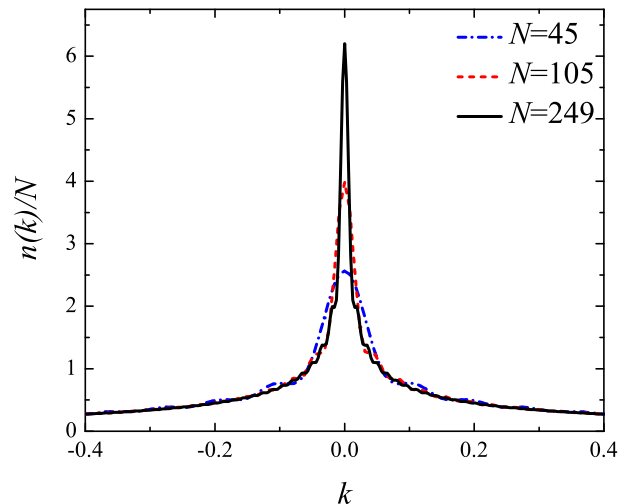


FIG. 9: (Color online) Normalized momentum density distributions for $N = 45$ (dash-dotted line), $N = 105$ (dashed line) and $N = 249$ (solid line) bosons in the incommensurate case, $N/M = 3/5$, when the periodic potential strength $\gamma = 2$. The momentum k is given in units of the inverse of the period of the periodic potential, $1/d$, and the momentum density is in units of the period of the periodic potential d .

The normalized momentum density distributions of periodically trapped TG gas in the incommensurate case are shown in Fig. 9 for various particle numbers. We see that, in the incommensurate case, the profiles of the normalized momentum density distributions become narrower with the increase of the system sizes, which is different from that in the commensurate case we discussed above. This is because in the incommensurate case, the system is a boson conductor, so the spatial distribution become more uniform as the system size increases due to many body repulsions of the particles. The small oscillations in the momentum profiles come from finite size effects and it will vanish in the thermodynamic limit. We do finite size scaling of zero-momentum peak with the particle number in the incommensurate case in Fig. 10, and we found, up to particle number $N = 249$, the zero-momentum peak $n(0) \propto N^\gamma$ with $\gamma = 1.51$. A universal relation among the scaling exponents of the ground-state occupation, the amplitude of the lowest natural orbital, and the zero-momentum peak height presented below shows that the exponent of the zero-momentum peak

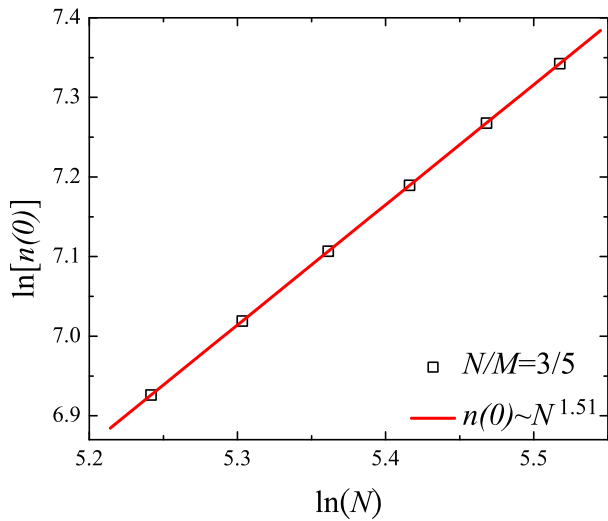


FIG. 10: (Color online) Zero-Momentum peak, $\ln[n(0)]$, as a function of particle number, $\ln(N)$, in the incommensurate case, $N/M = 3/5$, when the periodic potential strength $\gamma = 2$. $n(0)$ is in units of the period of the periodic potential d .

will converge to 1.5 for the incommensurate case in the thermodynamic limit.

To find a universal relation among various exponents presented above, we follow similar arguments of reference [24]. The zero momentum peak is calculated as

$$n(0) = (2\pi)^{-1} \int dx dx' \rho(x, x') \quad (36)$$

$$= (2\pi)^{-1} \int dx dx' \sum_j \lambda_j \phi_j(x) \phi_j(x') \quad (37)$$

$$= (2\pi)^{-1} \int dx dx' \lambda_0 \phi_0(x) \phi_0(x') \quad (38)$$

$$+ (2\pi)^{-1} \int dx dx' \sum_{j>0} \lambda_j \phi_j(x) \phi_j(x') \quad (39)$$

$$\propto \lambda_0 \int dx dx' \phi_0(x) \phi_0(x'). \quad (40)$$

Here we first express the SPRDM in the basis of natural orbitals where it is of a diagonal form. Then we discarded the contributions from higher orbitals since the occupations of higher orbitals are small. Meanwhile, the lowest orbital has even parity (no node) while the higher orbitals have node, so the integral of higher orbitals leads to cancellations.

If we define $n(0) \sim N^\gamma$, $\lambda_0 \sim N^\alpha$ and $\phi_0(x) \sim N^\beta$, then we have a universal relation among these exponents,

$$\gamma = \alpha - 2\beta. \quad (41)$$

Similar relation has been found in harmonically trapped hardcore boson gas [24]. However, we would like to stress that the scaling relation we found in Eq.(41) is more general, as it is valid for hardcore boson gas in various trapping potentials.

Scaling Exponents	α	β	γ
Ideal Bose gas	1	-0.5	2
Uniform TG gas[25, 33]	0.5	-0.5	1.5
Harmonically trapped TG gas[24, 25]	0.5	-0.25	1
Periodically trapped TG gas(Mott phase)	0	-0.5	1
Periodically trapped TG gas(Superfluid phase)	0.5	-0.5	1.5

TABLE II: Comparison of scaling exponents of the occupation number of the lowest orbital, the amplitude of the lowest orbital and the zero-momentum peak height for the TG gas in different trapping potentials.

We summarize the various scaling exponents for the hardcore bosons in different trapping potential in Table II. From Table II, we see that the scaling exponents of TG gas in different trapping potentials are quite different but these exponents are related to each other in a universal relation Eq. (41).

One may be confused why $n(0) \propto N^2$ rather than $n(0) \propto N$, for the ideal Bose gas, this comes from the difference between continuous case and discrete case,

$$\int n(k) dk = N, \quad (42)$$

while

$$\sum_k n_k = \sum_k \langle a_k^\dagger a_k \rangle = N. \quad (43)$$

So in the thermodynamic limit, where $N \rightarrow \infty, L \rightarrow \infty$ and $N/L \rightarrow \text{const}$, we have

$$n(k) = \frac{L}{2\pi} n_k \propto N n_k = N \langle a_k^\dagger a_k \rangle, \quad (44)$$

Therefore for the ideal gas,

$$n(0) \propto N \langle a_0^\dagger a_0 \rangle \propto N^2. \quad (45)$$

V. SUMMARY AND CONCLUSIONS

We have investigated the ground-state properties of a 1D TG gas trapped in a periodic potential. Based on the exact many-body wave function, obtained from Bose-Fermi mapping theorem, we have calculated the SPRDM numerically for systems containing more than 200 particles by employing the technique that the SPRDM can be expressed in a matrix product form in the TG gas limit. We have observed that, with the particle number increases, the SPRDM is almost diagonal which lacks ODLRO. The scaling analysis of the occupation numbers of the lowest orbital shows that there are no BEC for the periodically trapped TG gas both in the commensurate case and in the incommensurate case. We found that, in the commensurate case, the scaling exponents of the occupation numbers of the lowest orbital, the amplitude of

the lowest orbital and the zero-momentum peak height scale with the particle numbers are 0, -0.5 and 1 respectively, while are 0.5, -0.5 and 1.5 respectively in the incommensurate case. These exponents are related to each other by a simple relation.

Acknowledgments

We thank Prof. B. Wu and Y. F. Lo for valuable discussions. We are grateful to D. P. Zhang for his critical

reading of our manuscript. This work is supported by RGC Grant CUHK 402107 and CUHK 401108.

-
- [1] B. Paredes, A. Widera, V. Murg, O. Mandel, S. Fölling, I. Cirac, G. V. Shlyapnikov, T. W. Hänsch, and I. Bloch, *Nature (London)* **429**, 277 (2004).
 - [2] T. Kinoshita, T. Wenger, and D. S. Weiss, *Science* **305**, 1125 (2004).
 - [3] T. Kinoshita, T. R. Wenger, and D. S. Weiss, *Phys. Rev. Lett.* **95**, 190406 (2005).
 - [4] J. L. Roberts, N. R. Claussen, S. L. Cornish, E. A. Donley, E. A. Cornell, and C. E. Wieman, *Phys. Rev. Lett.* **86**, 4211 (2001).
 - [5] M. Girardeau, *J. Math. Phys.* **1**, 516 (1960).
 - [6] E. Lieb and W. Lineger, *Phys. Rev.* **130**, 1605 (1963).
 - [7] E. Lieb, *Phys. Rev.* **130**, 1616 (1963).
 - [8] M. D. Girardeau, *Phys. Rev.* **139**, B500 (1965).
 - [9] M. Olshanii, *Phys. Rev. Lett.* **81**, 938 (1998).
 - [10] D. S. Petrov, G.V. Shlyapnikov, and J. T. M. Walraven, *Phys. Rev. Lett.* **85**, 3745 (2000).
 - [11] V. Dunjko, V. Lorent, and M. Olshanii, *Phys. Rev. Lett.* **86**, 5413 (2001).
 - [12] L. Tonks, *Phys. Rev.* **50**, 955 (1936).
 - [13] V. I. Yukalov and M. D. Girardeau, *Laser Phys. Lett.* **2**, 375 (2005).
 - [14] T. Cheon and T. Shigehara, *Phys. Lett. A* **243**, 111 (1998); *Phys. Rev. Lett.* **82**, 2536 (1999).
 - [15] B. E. Granger and D. Blume, *Phys. Rev. Lett.* **92**, 133202 (2004).
 - [16] M. D. Girardeau and E. M. Wright, *Phys. Rev. Lett.* **84**, 5239 (2000).
 - [17] M. D. Girardeau and E. M. Wright, *Phys. Rev. Lett.* **84**, 5691 (2000).
 - [18] M. D. Girardeau, E. M. Wright, and J. M. Triscari, *Phys. Rev. A* **63**, 033601 (2001).
 - [19] K. K. Das, G. J. Lapeyre, and E. M. Wright, *Phys. Rev. A* **65**, 063603 (2002).
 - [20] M. D. Girardeau, K. K. Das, and E. M. Wright, *Phys. Rev. A* **66**, 023604 (2002).
 - [21] K. K. Das, M. D. Girardeau, and E. M. Wright, *Phys. Rev. Lett.* **89**, 170404 (2002).
 - [22] M. D. Girardeau and E. M. Wright, *Laser Phys.* **12**, 8 (2002).
 - [23] G. J. Lapeyre, M. D. Girardeau, and E. M. Wright, *Phys. Rev. A* **66**, 023606 (2002).
 - [24] T. Papenbrock, *Phys. Rev. A* **67**, 041601(R) (2003).
 - [25] P. J. Forrester, N. E. Frankel, T. M. Garoni, and N. S. Witte, *Phys. Rev. A* **67**, 043607 (2003).
 - [26] D. M. Gangardt, *J. Phys. A* **37**, 9335 (2004).
 - [27] A. Minguzzi and D. M. Gangardt, *Phys. Rev. Lett.* **94**, 240404 (2005).
 - [28] Y. Lin and B. Wu, *Phys. Rev. A* **75**, 023613 (2007).
 - [29] R. Pezer and H. Buljan, *Phys. Rev. Lett.* **98**, 240403 (2007).
 - [30] H. Buljan, K. Lelas, R. Pezer, and M. Jablan *Phys. Rev. A* **76**, 043609 (2007).
 - [31] J. Goold and Th. Busch, *Phys. Rev. A* **77**, 063601 (2008).
 - [32] X. Yin, Y. Hao, S. Chen, and Y. Zhang, *Phys. Rev. A* **78**, 013604 (2008).
 - [33] A. Lenard, *J. Math. Phys.* **5**, 930 (1964); *J. Math. Phys.* **7**, 1268 (1966).
 - [34] H. G. Vaidya and C. A. Tracy, *Phys. Rev. Lett.* **42**, 3 (1979).
 - [35] O. Penrose and L. Onsager, *Phys. Rev.* **104**, 576 (1956).
 - [36] C. N. Yang, *Rev. Mod. Phys.* **34**, 694 (1962).